Comparison of ^{3}He-, ^{4}He-, and ^{12}C-induced nuclear reactions in heavy-mass targets at medium excitation energies. II. Reaction model calculations*

K. J. Hofstetter and J. D. Stickler
Department of Chemistry, University of Kentucky, Lexington, Kentucky 40506
(Received 31 May 1973)

The excitation functions for neutron emission following fusion of ^{3}He, ^{4}He, and ^{12}C ions with a variety of heavy target nuclei, as determined in the previous communication, are compared to the statistical, exciton, and hybrid reaction model predictions. An initial exciton number of 5 is determined for α-particle-induced reactions by the simple exciton model. The initial exciton number of 7 is consistent with the ^{3}He-induced reactions by the exciton model. The hybrid-model predictions are found to be consistent with the ^{3}He- and ^{4}He-induced reactions using the initial exciton numbers of 3 and 4, respectively. The initial pre-equilibrium exciton states are assumed to be $2p$-$1n$ and $2p$-$2n$ pure particle states, respectively. The models permitting pre-equilibrium particle emission are not consistent with the data on ^{12}C-induced reactions; however, a statistical model calculation with level density parameter $a = A/20$ yields reasonable agreement with the cross sections. Angular momentum effects are discussed in terms of the model predictions and the isomer ratio for helion population of ^{186}Ir^g and ^{186}Ir^m are determined.

[NUCLEAR REACTIONS ^{197}Au(^{12}C,xn), ^{209}Bi(^{3}He,xn), ^{209}Bi(α,xn), ^{187}Re(^{3}He,xn), ^{187}Re(α,xn), ^{197}Au(^{3}He,xn) statistical model, exciton model, hybrid model, optical model, angular momentum; predict $\sigma(E)$ for (xn) reactions.]

I. INTRODUCTION

The experimental excitation functions for the neutron-emission reactions ^{197}Au(^{12}C, xn)$^{209-x}$At, ^{209}Bi(^{3}He, xn)$^{212-x}$At, ^{209}Bi(^{4}He, xn)$^{213-x}$At, ^{187}Re(^{3}He, xn)$^{190-x}$Ir, ^{187}Re(^{4}He, xn)$^{191-x}$Ir, and ^{197}Au(^{3}He, xn)$^{200-x}$Tl given in the previous paper,[1] are compared to the predictions of various nuclear reaction models. The statistical model, with[2] and without[3] the inclusion of angular momentum, is compared to the experimental excitation functions. The predictions of the equilibrium model with intermediate structure (exciton model), originally proposed by Griffin[4] and later modified by Blann,[5] are compared to the experimental excitation functions and the best value of the initial exciton number (N_i) is deduced. The equilibrium model permitting pre-equilibrium particle emission was later extensively modified by Blann[6] (the hybrid model), and is used to predict the above reaction excitation functions. The hybrid-model modifications included particle-hole distinguishability, proton and neutron distinguishability in the initial exciton state, and an energy-dependent pre-equilibrium emission fraction.

Due to the experimental errors described in Ref. 1, a comparison of the magnitudes of the predicted and experimental reaction cross sections could not always be used as the principal criterion for the model fits. In many cases, the best agreement is based on a comparison of the energy maximum, the full width at half maximum, or the general shape of the predicted versus experimental excitation functions.

II. REACTION MODEL CALCULATIONS

A. Predictions of the exciton model

The original equilibrium model with intermediate structure[4,5] was used in order to determine the most probable initial exciton number for the helion-induced nuclear reactions. This model involves the combination of the cross sections predicted by the statistical model and the cross sections predicted by the pre-equilibrium emission code.[7-9] The parameters involved in the pre-equilibrium calculation are the form of the particle-hole level density and the initial exciton number (N_i). The particle-hole-state density expression used in this calculation was based on the equal-spacing model where particles and holes were assumed indistinguishable.[4,5] In the statistical-model code, the form of the level density used in these computations is given by:

$$\omega(E^*) \propto \left(\frac{1}{E^*}\right)^2 \exp(2\sqrt{aE^*}),$$

where E^* is the excitation energy and the level-density parameter a was taken as $A/8$ consistent with a degenerate Fermi gas. The total reaction

TABLE I. Optical parameters used in the computation of the total and inverse reaction cross sections.

Projectile	$-V_0$ (MeV)	Form factor [a]	r_0 (fm)	a,b (fm)	$-W_0$ (MeV)	Form factor [a]	r_0 (fm)	a,b (fm)	$-V_{s.o.}$ (MeV)
Neutron [b]	$49.66-0.424E$ $-0.0042E^2$	WS	1.25	0.65	$1.5+4.35\ \ln E$	G	1.25	0.95	$12.0-1.79\ \ln E$
Proton [c]	$49.66-0.434E$ $0.0042E^2$	WS	1.25	0.65	$1.5+4.34\ \ln E$	G	1.25	1.2	$12.0-1.79\ \ln E$
α [d]	50.0	WS	1.17	0.567	21.0–23.0	WS	1.17	0.567	0.0
^{3}He [e]	$160-0.152E$ $+35(N-Z)/A$	WS	1.22	0.72	20.0–21.0	WS	1.5	0.86	0.0
^{12}C [f]	41.8	WS	1.26	0.49	16.4	WS	1.26	0.49	0.0

[a] WS stands for the Woods-Saxon form factor and G stands for the Gaussian form factor.
[b] From Ref. 12.
[c] From Ref. 13.
[d] From Ref. 14.
[e] From Refs. 15 and 16.
[f] From Ref. 17.

cross sections and inverse reaction cross sections were computed by standard optical-model codes, ABACUS[10] and SIGGMOPP.[11] The optical-model parameters used in this study were taken from the literature[12–17] and are reproduced in Table I. The ^{3}He parameters are a combination of those reported in Refs. 15 and 16. The ^{12}C-induced total reaction cross sections were computed by the square-well approximation given by Thomas[18] and found to agree with the optical-model prediction using the Auerbach and Porter parameters.[17] The separation energies of the emitted particles (restricted to p, n, and α particles) were computed using the table of nuclidic masses by Myers and Swiatecki.[19] The excitation energies at various bombarding energies are computed using the same mass tables.

The initial exciton number was varied between $N_i = 3$ and $N_i = 9$ for all reactions systems studied and the pre-equilibrium cross sections were determined. The statistical model calculation was also performed for all reaction systems. For each system studied, the statistical model and pre-equilibrium model predictions were combined by multiplying the pre-equilibrium cross sections by a constant fraction, referred to as the fraction of pre-equilibrium particle emission (FPE), and adding the result to the statistical model cross

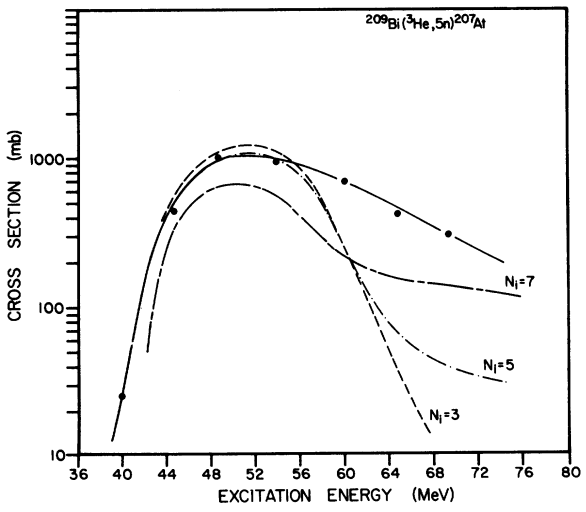

FIG. 1. The exciton model prediction of the ^{209}Bi-(^{3}He, $5n$)^{207}At reaction for initial exciton numbers 3, 5, and 7. The experimental curve is the solid line connecting the experimental data points.

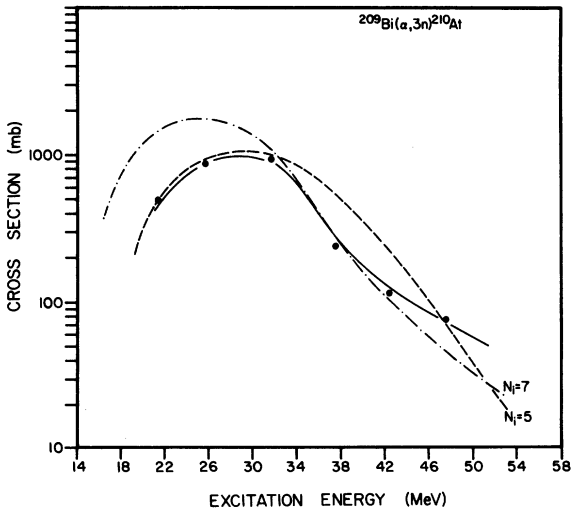

FIG. 2. The exciton model prediction of the ^{209}Be-(α, $3n$)^{210}At reaction for initial exciton numbers 5 and 7 as compared to the experimental excitation function.

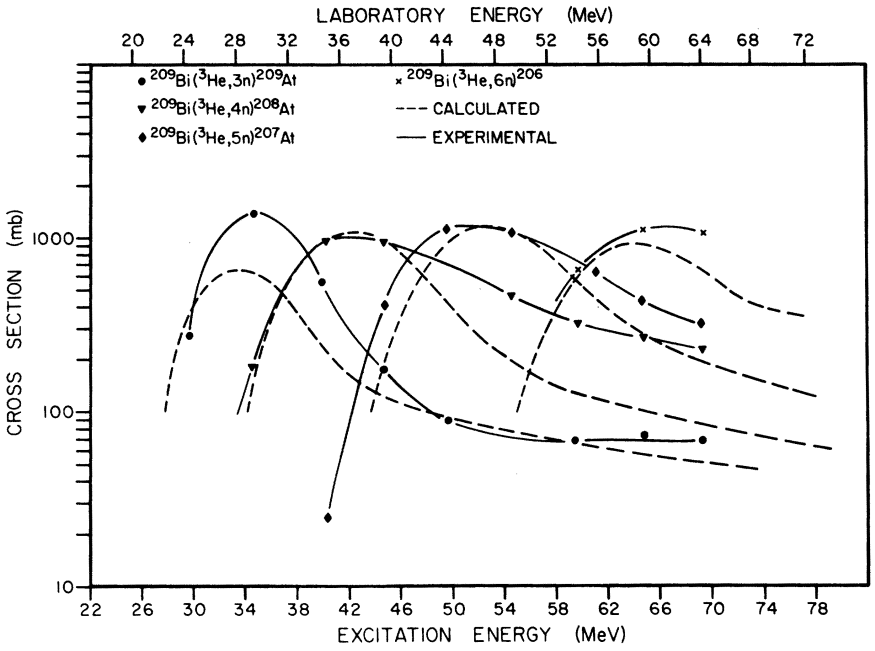

FIG. 3. A comparison of the experimental excitation functions for the ^{209}Bi-(^{3}He, xn)$^{212-x}$At reactions to the hybrid-model predictions using $N_i = 3$. Each dashed curve represents the hybrid-model prediction of the neutron-emission cross sections. The solid curve represents the experimental curve drawn through the experimental data points.

sections. The best value of the FPE for each reaction system was found by normalizing the pre-equilibrium cross sections to the experimental data at excitation energies where the equilibrium cross sections were very small. This normalization procedure was continued for each value of the initial exciton number for each reaction system studied. Detailed descriptions of these calculations are given in Refs. 7–9. The cross sections for all possible reactions were computed using the best values of N_i and FPE. In general, as the initial exciton number increased, the pre-equilibrium prediction approached the statistical model prediction; simultaneously, the FPE decreased.

Figure 1 shows the variation of the pre-equilibrium prediction of $N_i = 3, 5$, and 7 for the re-

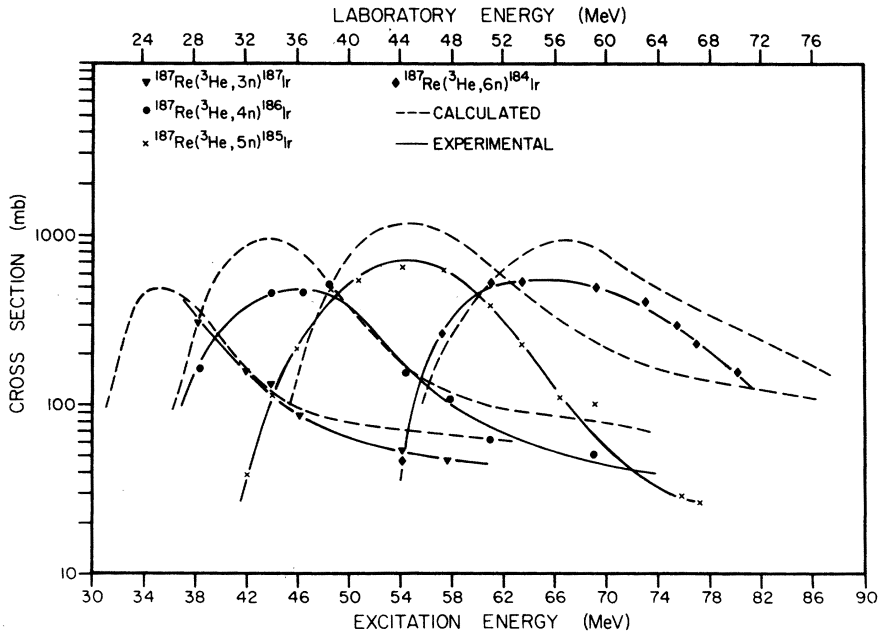

FIG. 4. A comparison of the experimental excitation functions for the ^{187}Re-(^{3}He, xn)$^{190-x}$Ir reactions to the hybrid-model predictions using $N_i = 3$.

action ^{209}Bi(^{3}He, $5n$)^{207}At. It can be seen that the energy maxima of the predicted cross sections are approximately the same for each value of the initial exciton number. The best agreement with the shape of the experimental excitation function is clearly the $N_i = 7$ prediction. Continuing this general procedure of optimization of parameters, led to the conclusion that $N_i = 7$ gave consistently the best agreement to the ^{3}He-induced reactions.

For the α-particle-induced reactions, the same fitting procedures were used comparing the computed cross sections to the experimental excitation functions. Figure 2 shows the predictions of $N_i = 5$ and 7 for the ^{209}Bi($\alpha, 3n$)^{210}At reaction. The figure indicates that $N_i = 5$ shows the best agreement to the experimental excitation function. In this case, the energy maximum of the excitation function is best reproduced by the $N_i = 5$ calculation. For the α-induced reactions on ^{209}Bi and ^{187}Re, the best agreement was found for $N_i = 5$. Lanzafame and Blann[9] and LeBeyec, Lefort, and Sarda[20] obtained the excitation functions for α-particle irradiations of ^{197}Au, ^{206}Pb, and ^{208}Pb, respectively. These investigators found that an initial exciton number of 5 yielded best agreement to the experimental excitation functions. Cline and Blann[7] have shown that with the inclusion of particle-hole distinguishability in the initial exciton state, most ^{4}He-induced reactions are best described with an initial exciton number of 5. This conclusion was based on fits to excitation functions and emitted-particle energy spectra.

The excitation functions for the ^{12}C-induced reaction on ^{197}Au were computed via the above technique. In general, there was poor agreement between the predicted and experimental cross sections. The trend was for a small value of FPE and large initial exciton number. The best agreement was found by just considering the pure statistical calculation without a pre-equilibrium emission component (cf., Sec. C).

B. Predictions of the hybrid model

Blann[6,21] modified the simple exciton model by including neutron-proton and particle-hole distinguishability in the initial exciton state using the intermediate-state densities given in Ref. 21. The FPE was eliminated as a parameter by including an energy-dependent FPE. The pre-equilibrium model cross sections and the statistical model cross sections, using $a = A/8$, are then combined formally. This combined calculation, referred to as the hybrid model, was used to compute the cross sections for the reaction systems reported in this study.

Blann and Mignerey[22] have shown that the hybrid model can be successfully applied to emitted-particle kinetic-energy spectra. It was reported that the α-particle-induced reactions were best described with an initial exciton number of 4. The initial exciton state was a pure four-particle state composed of two protons and two neutrons. The hybrid-model code was used to compute the cross sections for the ^{4}He-induced reactions observed in this study using this type of initial exciton state (i.e., a pure four-particle state comprised of two protons and two neutrons). For the ^{3}He-induced reactions, the initial exciton number was taken to be a three-particle state with two protons and one neutron. The predicted excitation functions and experimental cross sections for each helion-induced reaction reported in Ref. 1 are shown in Figs. 3–7.

Figure 3 shows the predicted and the experimental excitation functions for the ^{209}Bi(^{3}He, xn)-$^{212-x}$At reactions where $x = 3, 6$ using an initial exciton number of 3. The over-all agreement between the hybrid-model predictions (shown by dashed curves) and the experimental cross sections is good with the exception of the (^{3}He, $4n$) reaction. There is a significantly large high-energy tail to this excitation function, which cannot be simply an error in the branching ratio.

Figure 4 is a graph of the xn reactions induced by ^{3}He ions on ^{187}Re. The hybrid-model calculation with $N_i = 3$ is shown with the experimental data for the $3n$, $4n$, $5n$, and $6n$ reactions. Consistently low values of experimental cross sections probably reflect errors in the branching ratios of the isotopes.

Figure 5 shows the excitation functions for the $3n$, $4n$, $5n$, and $6n$ reactions produced by the bombardment of ^{197}Au with ^{3}He ions. The hybrid-model predictions with $N_i = 3$ are shown. The magnitudes of the cross sections are not in good agreement which again could be due to branching ratio errors. The energy maxima and shapes of the experimental excitation functions are well reproduced by the hybrid-model calculation.

Figure 6 displays the experimental excitation functions for the ^{187}Re(α, xn)$^{191-x}$Ir reactions where $x = 3$–7. The hybrid-model prediction is shown with $N_i = 4$. Of these excitation functions, only that for the $3n$ reaction seriously deviates from the model predictions of energy maxima and general shapes. The experimental $3n$ excitation function seems to be seriously affected by the Coulomb barrier. The peak of the experimental $4n$ excitation function is somewhat broader than its predicted value. The $5n$ cross section is systematically high but fits the position and shape of the predicted excitation function. There is good agreement for the $6n$ reaction.

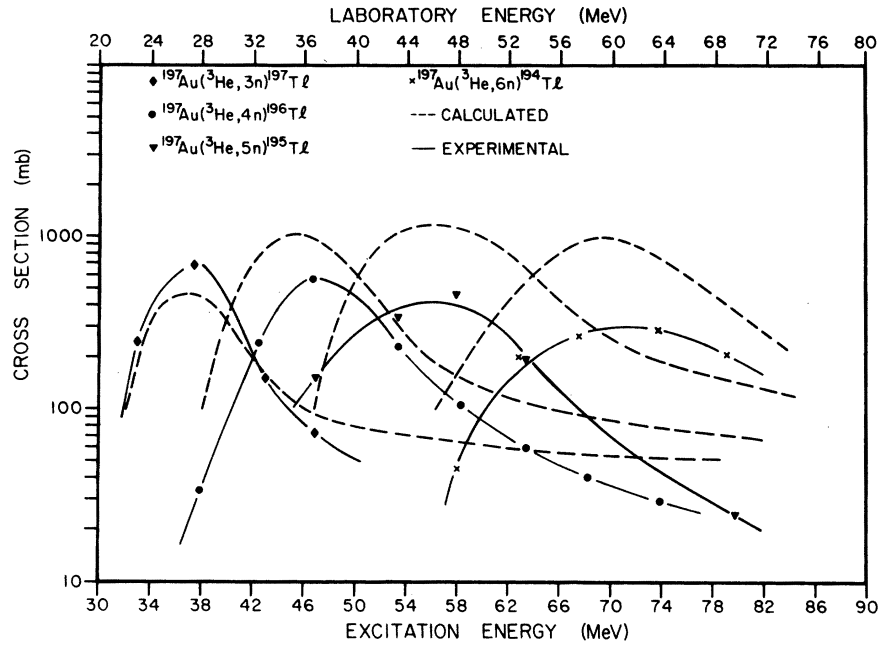

FIG. 5. A comparison of the experimental excitation functions for the ^{197}Au-(^{3}He, xn)$^{200-x}$Tl reactions to the hybrid-model predictions using $N_i = 3$.

Figure 7 shows the α-induced neutron-emission reactions on ^{209}Bi. Except for the $2n$ reaction, the experimental cross sections are in good agreement with the hybrid-model prediction using $N_i = 4$. The low value of $2n$ reaction cross sections is most certainly a branching-ratio problem. The $3n$, $4n$, $5n$, and $6n$ reactions show reasonable agreement to the hybrid-model prediction of excitation-function shapes and energy maxima.

No attempts were made to fit the experimental excitation functions with variation of parameters in the hybrid-model calculation. Blann and Mignerey[22] show that for proton-induced reactions, the best fit to emitted-particle spectra was found when $N_i = 2$, a pure two-particle state. A more reasonable initial excitation state was taken to be $N_i = 3$, a two-particle–one-hole state using free-scattering (n, p) and (p, p) cross sections to ob-

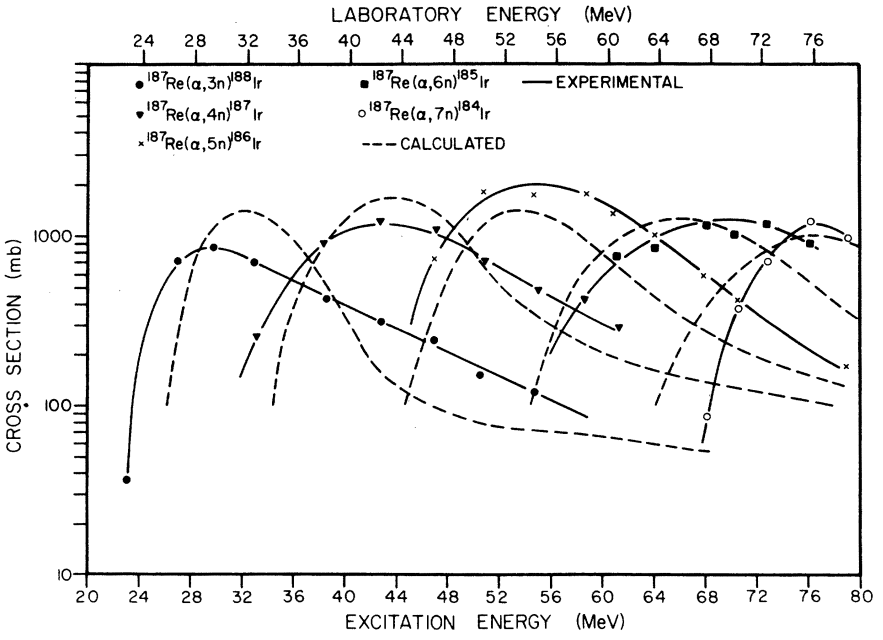

FIG. 6. A comparison of the experimental excitation functions for the ^{187}Re-(α, xn)$^{191-x}$Ir reactions to the hybrid-model predictions using $N_i = 4$.

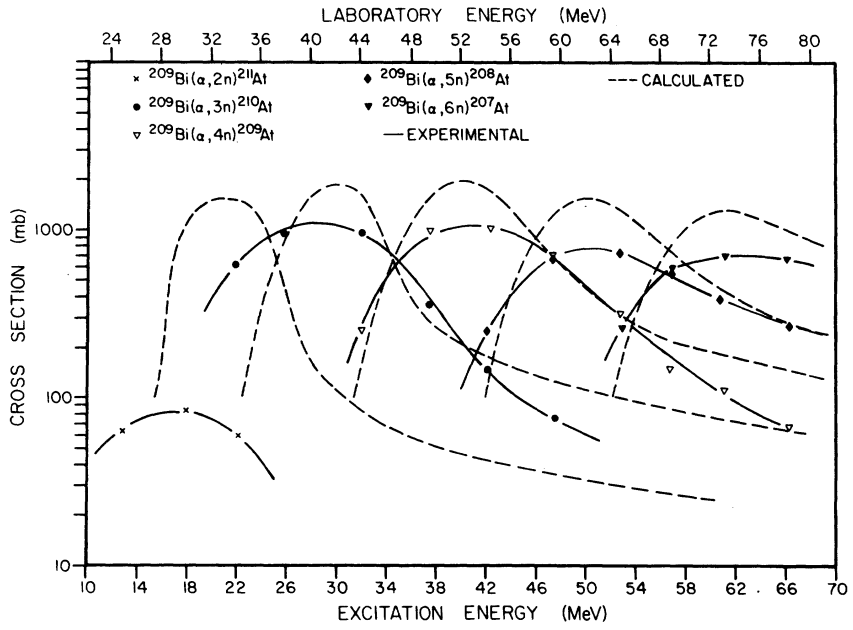

FIG. 7. A comparison of the experimental excitation functions for the ^{209}Bi-$(\alpha, xn)^{213-x}$At reactions to the hybrid-model predictions using $N_i = 4$.

tain the division between neutrons and protons in the initial 2p1h state. Such a state was used in their hybrid-model code, however the predictions did not agree with the data reported in Ref. 22.

Because of the experimental errors associated with the cross sections reported in Ref. 1, no information on the character of the initial exciton state could be deduced by variation of parameters in the hybrid model. For example, the ^{3}He-induced reactions were compared to hybrid-model predictions using $N_i = 5$ where the initial exciton state was 4p1h in nature and the particle state was assigned 40% neutron and 60% proton character. The predicted results showed the tails of the excitation functions were lowered (~30%) and the balance of the cross section was put in the lower portion of the excition function. The magnitudes of the changes, in light of the experimental errors, were such that no definitive conclusion could be drawn regarding the quality of fit.

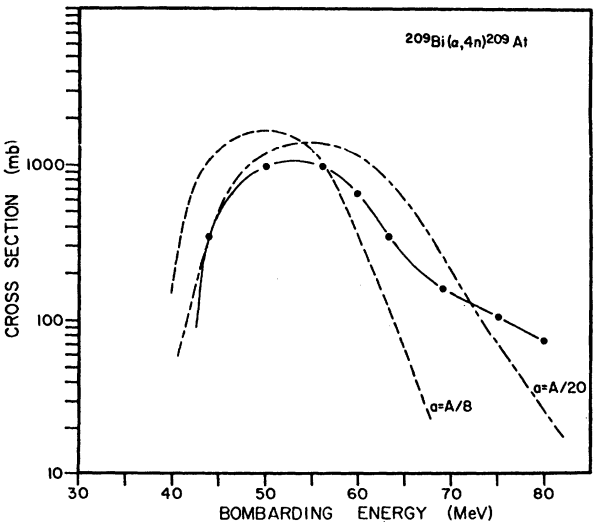

FIG. 8. The experimental excitation function for the ^{209}Bi$(\alpha, 4n)^{209}$At reaction as compared to the statistical-model predictions with $a = A/8$ and $a = A/20$.

C. Predictions of the statistical model

All experimental excitation functions were compared to the statistical-model predictions using the form of the level density given by Weisskopf and Ewing.[3] The same criteria (cf., Sec. I) were used to fit the data to the model predictions. The level-density parameter was varied for values between $A/4$ and $A/25$. Figure 8 shows the results of the statistical-model calculation for $a = A/8$ and $a = A/20$ as compared to the experimental data for the ^{209}Bi$(\alpha, 4n)^{209}$At reaction. The fit to this excitation function is typical for the helion-induced reactions reported in this study. As can be seen from the figure, the level-density parameter $a = A/20$ gives best agreement to the experimental data. The inclusion of angular momentum in the statistical-model calculation for helion-induced reactions produced a slight energy shift in the peak of the excitation function to higher energy and increased the full width at half maximum (FWHM). The magnitudes of these changes were well within the experimental-data error limits. The high-energy tailing of the experimental data has long

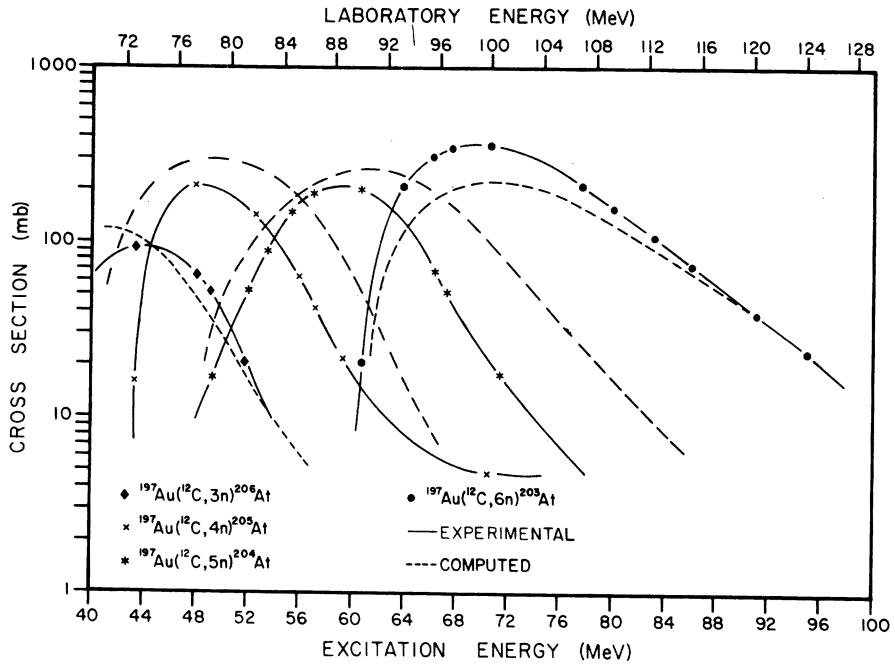

FIG. 9. A comparison of the experimental excitation functions for the ^{197}Au-(^{12}C, xn)$^{209-x}$At reactions to the statistical-model predictions using $a = A/20$.

been attributed to a direct-reaction component. The statistical calculation could not reproduce the hard component in the excitation functions. In order to fit our helion-induced cross-section data, a level-density parameter of $a = A/20$ was required to best reproduce the energy maxima and FWHM of the excitation functions. The resulting reduction in level density is not consistent with a degenerate Fermi gas. It appears that the fermi-gas statistical model can only be confidently applied to helion-induced nuclear reactions when a pre-equilibrium emission component is added to the initial state.

As mentioned previously, the ^{12}C-induced reactions on ^{197}Au did not seem to follow the predictions of the pre-equilibrium models. The statistical model with the angular-momentum-dependent level density given by Lang and LeCouteur[2] was used to predict the cross sections for the (xn) reactions. The level-density parameter of $a = A/20$, used in the statistical-model computation, was found to best fit the experimental data for the $3n$, $4n$, $5n$, and $6n$ excitation functions. Figure 9 is a comparison of the experimental data to the statistical-model predictions using $a = A/20$. As can be seen from the figure, the over-all agreement between the experimental cross sections and computed excitation functions is very good. There does not seem to be significant high-energy tailing to the experimental excitation functions suggesting a small direct-reaction component to the (xn) reactions. This can be qualitatively understood from the standpoint of the high angular momentum brought into the compound nucleus. Levels are populated above the yrast line and significant rotational energy becomes unavailable for nucleon emission and must be carried off by photons.[23]

It appears that the helion- and ^{12}C-induced reactions reported in this study are both consistent with $a = A/20$. This reduction in the number of degrees of freedom for the equilibrium system is not consistent with the pure statistical model. While pre-equilibrium particle emission can successfully account for the hard component of the helion-induced reaction data, the (^{12}C, xn) data show no such component. It is planned to determine the effect of changing the moment of inertia from its rigid-body value, assumed in these computations. It has been reported by Obst *et al.*[24] that ^{16}O-induced reactions on medium-mass targets can be described by a pure statistical-model calculation when the moment of inertia is one half the rigid-body value. Another approach would be to use the Hauser-Feshbach method as described by Eberhardt *et al.*[25] Both of the computations will be performed and presented in a subsequent communication.[26]

D. Angular momentum effects

At one given excitation energy, the angular momentum transferred into the fused nuclear system by the incoming projectile will increase in the order: ^{3}He, ^{4}He, ^{12}C at energies above the Cou-

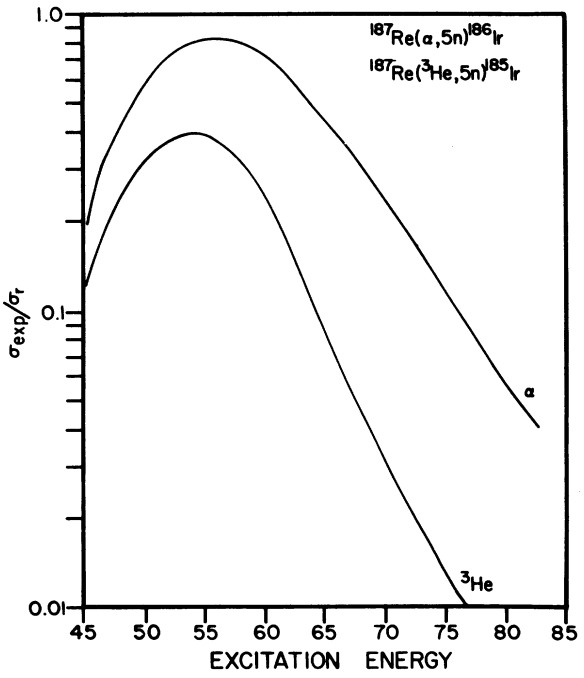

FIG. 10. A comparison of the ratios of the experimental excitation function (σ_{exp}) to the total reaction cross section (σ_r) for the ^{187}Re(^{3}He, $5n$)^{185}Ir and ^{187}Re-(α, $5n$)^{186}Ir reactions.

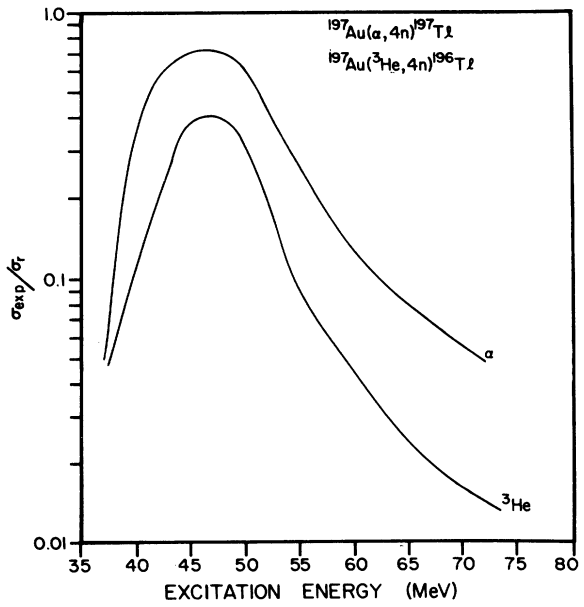

FIG. 11. A comparison of the ratios of the experimental functions to the total reaction cross sections for the ^{197}Au(^{3}He, $4n$)^{196}Tl and ^{197}Au(α, $4n$)^{197}Tl reactions.

lomb barrier for the systems under investigation. The ratio of the experimentally measured cross sections for each system studied were computed. In Fig. 10 is shown a comparison of the ^{187}Re-(^{3}He, $5n$)^{185}Ir and the ^{187}Re(α, $5n$)^{186}Ir reactions. As can be seen from the figure, there are no appreciable differences in the shapes of the excitation functions. Using the procedure of Alexander and Simonoff,[27] the average excitation energies for the $5n$ reactions induced by ^{3}He and ^{4}He on ^{187}Re were found to be 56.2 and 58.9 MeV, respectively. The average angular momentum brought into the nuclear system by the ^{3}He and ^{4}He at these excitation energies are 12.0 and 17.6 units. In Fig. 11 is shown the ^{197}Au(^{3}He, $4n$)^{196}Tl and ^{197}Au-(α, $4n$)^{197}Tl reactions. The data on the α-particle irradiation of ^{197}Au were taken from Blann and Lanzafame.[9] Again, there seem to be no appreciable differences in the shapes of the excitation functions. The average excitation energies are 49.7 and 50.8 MeV for the ^{3}He and α-induced reactions, respectively. This corresponds to an average spin of the compound nuclei of 10.3 and 15.6 units.

In Fig. 12 is a comparison of the ^{209}Bi(^{3}He, $5n$)-^{207}At, ^{209}Bi(α, $5n$)^{208}At, and ^{197}Au(^{12}C, $5n$)^{204}At reactions. Once again the shapes of the helion-induced $5n$ reactions are similar while the (^{12}C, $5n$) reaction is shifted to higher energy and is much narrower in shape. The average excitation energies of the compound nuclei following fusion with

TABLE II. A comparison of the average excitation energies $\langle E^* \rangle$, the energy available for nucleon and photon emission ($\langle E^* \rangle - \sum_i B_i$), and the average angular momentum $\langle J \rangle$ of the compound system for the $4n$ and $5n$ reactions observed in this study.

Reaction	$\langle E^* \rangle$ [a] (MeV)	$\left(\langle E^* \rangle - \sum_i B_i\right)$ [a] (MeV)	$\langle J \rangle$ [a]
^{209}Bi(^{3}He, $4n$)	48.2	18.8	11.1
^{197}Au(^{3}He, $4n$)	49.7	17.5	10.3
^{187}Re(^{3}He, $4n$)	46.2	16.8	9.1
^{209}Bi(α, $4n$)	43.8	16.7	15.9
^{197}Au(α, $4n$) [b]	50.8	20.1	15.6
^{187}Re(α, $4n$)	46.0	17.2	14.4
^{197}Au(^{12}C, $4n$)	50.2	17.7	21.0
^{209}Bi(^{3}He, $5n$)	54.6	18.1	12.8
^{197}Au(^{3}He, $5n$)	58.1	19.6	12.5
^{187}Re(^{3}He, $5n$)	56.2	19.9	12.0
^{209}Bi(α, $5n$)	55.3	19.6	18.7
^{197}Au(α, $5n$) [b]	61.5	22.1	17.5
^{187}Re(α, $5n$)	58.9	21.8	17.6
^{197}Au(^{12}C, $5n$)	58.6	16.9	27.2

[a] Computed by the technique described in Ref. 24.
[b] Computed from the cross sections reported by Blann and Lanzafame (Ref. 8).

^{3}He, ^{4}He, and ^{12}C ions are 54.6, 55.3, and 58.6 MeV with average angular momenta of 12.8, 18.7, and 27.2 units, respectively.

The systematic trend suggested by these data is that the average excitation energy for a particular xn reaction increases in order: ^{3}He, ^{4}He, ^{12}C. Table II gives the average excitation energy $\langle E^* \rangle$, the energy available for neutron and photon emission ($\langle E^* \rangle - \sum_i B_i$) ($B_i$ is the binding energy of the evaporated neutron), and the average angular momentum for the compound nucleus $\langle J \rangle$ for the $4n$ and $5n$ reactions observed in this study. Using the rigid-body moment of inertia, the magnitudes of the energy shifts can be accounted for by subtracting the rotational energy from the available excitation energy. The relatively small amounts of angular momentum brought in by the ^{3}He ion could efficiently be carried off by neutron evaporation.[28] The data would also suggest that (^{3}He, xn) reactions should not show a strong population of the ground-state rotational band of the product nuclei. The α-particle-induced reactions may have significant γ-ray competition early in the decay cascade due to the low density of residual states and the γ rays preferentially seek out the ground-state rotational cascade. The ^{12}C-induced reactions should have more γ-ray competition early in the decay cascade and consequently populate levels high in the ground-state rotational band.

Isomer ratio results were measured for helion population of ^{186}Ir (spin 5)[29] and ^{186}Ir^m (spin 2)[30] by the ^{187}Re(^{3}He, $4n$)^{186}Ir and ^{187}Re(α, $5n$)^{186}Ir reactions. Plots of the isomer ratios are given in Fig. 13. The slopes of the lines are consistent with the increased population of the high-spin isomer with increasing angular momentum of the compound system. The slope of the ^{3}He-induced reaction is much less, qualitatively suggesting that the neutrons carry off much of the angular momentum brought in to the system. Other isotopes which have metastable states had isomeric radiations which were contaminated with radiations from other isotopes or the half-life was too short to be detected under the conditions of this study.

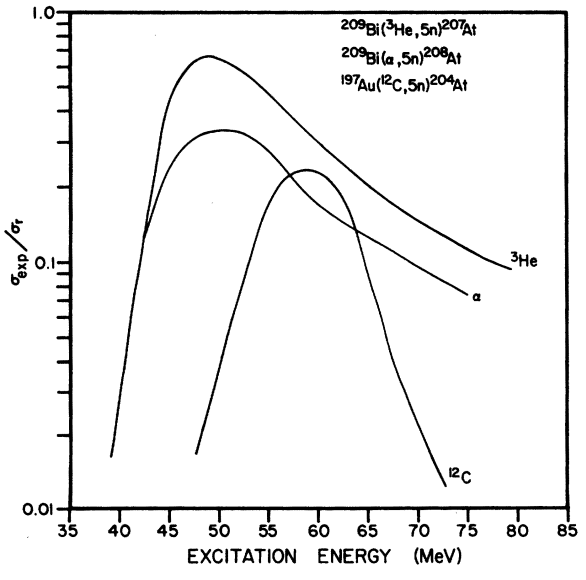

FIG. 12. A comparison of the ratios of the experimental excitation functions to the total reaction cross sections for the ^{209}Bi(^{3}He, $5n$)^{207}At, ^{209}Bi(α, $5n$)^{208}At, and ^{197}Au(^{12}C, $5n$)^{204}At reactions.

E. Total reaction cross sections

A sensitive test of the optical-model parameters chosen for computing the total reaction cross section would be to measure the cross sections for all possible reactions. The experiments described in this study were not optimized to measure the cross sections for all reactions, however. A comparison of the fusion cross sections which lead to neutron emission is typically made to the predicted total reaction cross section. Such a comparison of these data was made and systematic deviations were observed at high excitation energies. The cross sections for many of the 6, 7, and $8n$ reactions could not be determined due to the short half-lives of the product isotopes and would cause such a deviation.

Table III gives the fraction of the total reaction cross section (fn) which proceeds by neutron

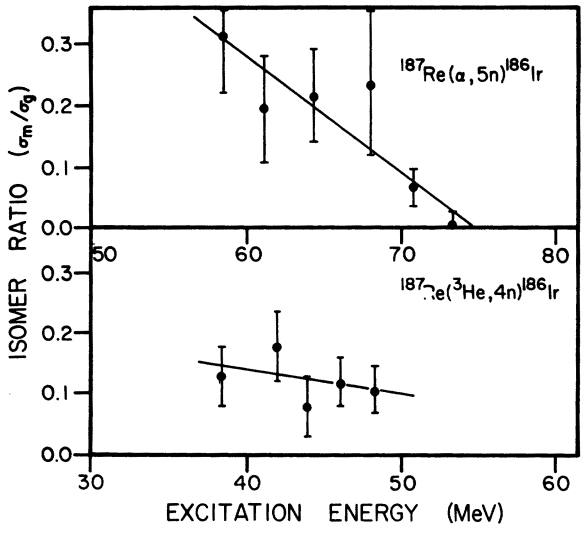

FIG. 13. A comparison of the isomer ratios for populating ^{186}Ir^m (spin 2) and ^{186}Ir^g (spin 5) by the ^{187}Re(α, $5n$)-^{186}Ir and ^{187}Re(^{3}He, $4n$)^{186}Ir reactions.

TABLE III. A comparison of the fraction of the total reaction cross section which proceeds by neutron emission (fn) versus the fraction computed by the statistical [$fn(S)$] and hybrid [$fn(H)$] models.

Reaction	E^* (MeV)	fn [a]	$fn(S)$ [b]	$fn(H)$
^{197}Au(^{12}C,xn)	60.7	0.31(7) [c]	0.73	
	60.7	0.54 [d]		
^{209}Bi(^{3}He,xn)	60.3	0.84(12)	0.67	0.70
^{187}Re(^{3}He,xn)	50.8	0.60(10)	0.75	0.84
^{197}Au(^{3}He,xn)	37.5	0.77(13)	0.98	0.78
^{209}Bi(α,xn)	42.2	0.62(11) [e]	0.75	0.84
^{187}Re(α,xn)	61.2	0.83(12)	0.68	0.80

[a] Computed by dividing the $\sum\sigma(xn)$ by the total reaction cross section.

[b] Computed using $a=A/20$.

[c] The total reaction cross section was corrected for fission competition by subtracting the fission cross sections reported by G. E. Gordon, A. E. Larsh, T. Sikkeland, and G. T. Seaborg, Phys. Rev., 120, 1341 (1960). The number in parentheses is the experimental error in fn.

[d] Fraction computed from the (^{12}C,xn) data of R. Bimbot, M. Lefort, and A. Simon, J. Phys. (Paris) 29, 563 (1968).

[e] The total reaction cross section corrected for fission cross section from A. Khodai-Joopari, R. C. Gatti, and S. G. Thompson, UCRL Report No. UCRL-16580, 1966 (unpublished).

emission. In cases where the total fission cross sections had been measured, the total reaction cross section was corrected for fission competition. The resulting fraction is then a measure of the number of neutrons emitted per reaction cascade. Because of the systematic deviations reported previously, the excitation energies chosen for each reaction were based on the maxima in the total neutron-emission cross sections. Also reported in this table are the results of the statistical- and hybrid-model predictions of the neutron-emission fractions. As expected, the statistical-model calculation predicts high neutron-emission probability at low excitation energies and decreases appropriately with increasing excitation energy.

As stated in the previous paper, there are probably significant errors in the branching ratios of the isotopes produced in this study which would seriously affect these computations. The trend in the data, however, would suggest that charged-particle emission competes at low excitation energies, consistent with the hybrid-model predictions.

III. SUMMARY AND CONCLUSION

The helion-induced reaction systems presented in this study show good agreement to the equilibrium reaction models with intermediate structure. The simple exciton model is found to fit the ^{3}He- and ^{4}He-induced reactions using initial exciton numbers of 7 and 5, respectively. The hybrid-model predictions, where the initial exciton state is given more definite structure, are consistent with the experimental helion-induced excitation functions when the initial exciton state is given the particle character of the incident helion. The equilibrium models permitting pre-equilibrium particle emission do not describe the ^{12}C-induced reactions, probably because of the high angular momentum of the compound state. A statistical-model calculation including angular-momentum-dependent level densities with $a=A/20$ reproduces the shapes and energy maxima of the (^{12}C,xn) reactions. Comparing the ^{3}He-, α-, and ^{12}C-induced reactions suggests that angular momentum effects are playing an important role in the deexcitation of the fused state. Isomer ratio studies are in progress to reveal differences in the ^{3}He and ^{4}He reaction paths to deduce the angular momentum of the final product state. If the neutrons carry off almost all of the angular momentum brought in by ^{3}He ions, then the population ratio of two isomers, which differ by several units of angular momentum, should be relatively insensitive to excitation energy.

ACKNOWLEDGMENTS

The authors would like to express their appreciation to Marshall Blann of the University of Rochester for lending his computer programs and helpful advice. R. Hahn, K. Toth, and E. Newman also provided stimulating comments. The help of L. Thrailkill and the staff at the University of Kentucky Computing Center is gratefully acknowledged.

*From the Ph.D. thesis of J. D. Stickler, University of Kentucky, 1973.

[1] J. D. Stickler and K. J. Hofstetter, preceding paper, Phys. Rev. C 9, 1064 (1974).

[2] J. M. B. Lang and K. J. LeCouteur, Proc. Phys. Soc. 67A, 586 (1964).

[3] V. F. Weisskopf and D. H. Ewing, Phys. Rev. 57, 742 (1940).

[4] J. J. Griffin, Phys. Rev. Lett. 17, 545 (1966).

[5] M. Blann, Phys. Rev. Lett. 21, 1357 (1968).

[6]M. Blann, Phys. Rev. Lett. 27, 337 (1971).
[7]C. K. Cline and M. Blann, Nucl. Phys. A172, 225 (1971).
[8]W. W. Bowman and M. Blann, Nucl. Phys. A131, 513 (1969).
[9]M. Blann and F. M. Lanzafame, Nucl. Phys. A142, 559 (1970).
[10]E. H. Auerbach, N. C. Francis, D. T. Goldman, and C. R. Lubitz, Knolls Atomic Power Laboratory Report No. KAPL-3020, 1964 (unpublished).
[11]E. R. Parkinson, Ph.D. dissertation, University of Washington, 1965 (unpublished).
[12]G. S. Mani, M. A. Melkanoff, and I. Iori, Centre d'Etudes Nucleaire Report No. CEA-2380, 1963 (unpublished).
[13]G. S. Mani, M. A. Melkanoff, and I. Iori, Centre d'Etudes Nucleaire Report No. CEA-2379, 1963 (unpublished).
[14]J. R. Huizenga and G. Igo, Nucl. Phys. 29, 462 (1962).
[15]N. E. Scott, J. W. Cobble, and P. J. Daly, Nucl. Phys. A119, 131 (1968).
[16]F. D. Becchetti and G. W. Greenless, Phys. Rev. 182, 1190 (1969).
[17]E. H. Auerbach and C. E. Porter, in *Proceedings of the Third Conference on Reactions Between Complex Nuclei, Asilomar, 1963*, edited by A. Ghiorso and R. M. Diamond (Univ. of California Press, Berkeley, 1963), p. 19.
[18]T. D. Thomas, Phys. Rev. 116, 137 (1959).
[19]W. D. Myers and W. J. Swiatecki, UCRL Report No. UCRL-11980, 1965 (unpublished).
[20]Y. LeBeyec, M. Lefort, and M. Sarda, Nucl. Phys. A192, 405 (1972).
[21]M. Blann, Phys. Rev. Lett. 28, 757 (1972).
[22]M. Blann and A. Mignerey, Nucl. Phys. A186, 245 (1972).
[23]D. G. Sarantites, Nucl. Phys. A93, 567 (1967).
[24]A. N. Obst, D. L. McShan, M. B. Greenfield, R. Holub, and R. H. Davis, Phys. Rev. C 8, 1379 (1973).
[25]K. A. Eberhard *et al.*, Nucl. Phys. A120, 673 (1969).
[26]K. J. Hofstetter and R. Holub, to be published.
[27]J. M. Alexander and G. N. Simonoff, Phys. Rev. 133, B93 (1964).
[28]T. D. Thomas, ORNL Report No. CONF-720669, 1972 (unpublished), p. 148.
[29]K. J. Hofstetter, D. S. Brenner, and T. T. Sugihara, Phys. Rev. C 8, 2442 (1973).
[30]M. Finger *et al.*, CERN Report No. CERN 70-29, 1970 (unpublished).